# Ultralarge multimers of von Willebrand factor form spontaneous high-strength bonds with the platelet glycoprotein Ib-IX complex: studies using optical tweezers

Maneesh Arya, Bahman Anvari, Gabriel M. Romo, Miguel A. Cruz, Jing-Fei Dong, Larry V. McIntire, Joel L. Moake, and José A. López

**Ultralarge von Willebrand factor (ULVWF) multimers have been implicated in the pathogenesis of the catastrophic microangiopathic disorder, thrombotic thrombocytopenic purpura. Spontaneous ULVWF binding to platelets has been ascribed to increased avidity due to the greatly increased number of binding sites for platelets (the A1 domain) per molecule. To address the mechanism of enhanced ULVWF binding to platelets, we used optical tweezers to study the unbinding forces from the glycoprotein Ib-IX (GP Ib-IX) complex of plasma VWF, ULVWF, and isolated A1 domain. The unbinding force was defined as the minimum force required to pull ligand-coated beads away from their attachment with GP Ib-IX–expressing cells. Beads coated with plasma VWF did not bind to the cells spontaneously, requiring the modulators ristocetin or botrocetin. The force required to break the ristocetin- and botrocetin-induced plasma VWF–GP Ib-IX bonds occurred in integer multiples of 6.5 pN and 8.8 pN, respectively, depending on the number of bonds formed. In contrast, beads coated with either ULVWF or A1 domain bound the cells in the absence of modulators, with bond strengths in integer multiples of approximately 11.4 pN for both. Thus, in the absence of shear stress, ULVWF multimers form spontaneous high-strength bonds with GP Ib-IX, while plasma VWF requires exogenous modulators. The strength of individual bonds formed with GP Ib-IX was similar for both ULVWF and the isolated A1 domain and greater than those of plasma VWF induced by either modulator. Therefore, we suggest that the conformational state of ULVWF multimers is more critical than their size for interaction with platelets. (Blood. 2002; 99:3971-3977)**



## Introduction

Platelet thrombi form in the arterial circulation following injury and desquamation of the endothelial cells. At arterial shear stresses, platelet attachment to the vessel wall is initiated by the binding of platelet glycoprotein (GP) Ib-IX-V complexes to von Willebrand factor (VWF) multimers in the subendothelium. As a result, platelets tether, roll, and then adhere firmly to the subendothelium. This adhesion subsequently initiates a complex sequence of events that includes platelet activation, secretion, and cohesion.[1-5]

The GP Ib-IX-V complex is made up of 4 polypeptide chains: GP Ibα, GP Ibβ, GP IX, and GP V. Each is a member of the leucine-rich repeat superfamily of proteins,[1] characterized by the presence of a motif containing either one copy or tandem repeats of a 24–amino acid sequence with conserved spacing of leucines. GP Ibα is disulfide-linked to GP Ibβ to form GP Ib; GP IX and GP V noncovalently associate with GP Ib. GP Ibα contains the VWF-binding domain, located within the leucine-rich repeat–containing N-terminal sequence of the polypeptide. The GP Ib-IX-V complex mediates platelet adhesion by binding VWF within a region encompassed by a disulfide bond between Cys509 and Cys695 known as the A1 domain, 1 of 3 conserved A domains in VWF.[6]

VWF is a multimeric glycoprotein synthesized in endothelial cells and megakaryocytes from which it is secreted constitutively or stored in granules, the α-granules of megakaryocytes and platelets, and the Weibel-Palade bodies of endothelial cells. The multimers are formed within the endoplasmic reticulum by N-terminal disulfide linkage of dimers initially joined by C-terminal disulfide bonds, which results in long chains of VWF polypeptides linked in head-to-tail, then tail-to-head, orientation.[6,7] The resultant multimers are very heterogeneous in size, essentially forming a multimer ladder, with the molecular masses of successive multimers differing by the mass of a VWF dimer. Upon either constitutive or stimulated secretion, VWF undergoes an additional processing step in the plasma, with ultralarge VWF (ULVWF) multimer adhesive forms being converted to smaller forms by the action of a plasma metalloprotease.[8]

Although plasma VWF multimers are continuously in contact with platelets, the platelet–VWF interaction cannot be detected in circulating blood under normal conditions. In contrast, platelets will attach to immobilized VWF multimers under the conditions of elevated shear stress present in the normal arterial and arteriolar circulation.[9,10] With pathologically elevated shear stresses, as in regions of arterial stenosis, large plasma VWF multimers attach to the platelets, with consequent activation and aggregation of the platelets. ULVWF multimers are more active than the largest plasma VWF multimers in promoting these interactions.[11] Evidence exists supporting a shear-induced conformational alteration

From the Department of Bioengineering, Rice University; and the Division of Thrombosis Research, Department of Medicine, Baylor College of Medicine, Houston, TX.

Submitted November 19, 2001; accepted January 22, 2002. Prepublished online as *Blood* First Edition Paper, April 17, 2002; DOI 10.1182/blood-2001-11-0060.

Supported by National Institutes of Health grants 1P50 HL65967 and NS23327; the Robert A. Welch Foundation grant no. C938; a grant-in-aid from the American Heart Association–Texas Affiliate; and Special Opportunity and Development Awards from The Whitaker Foundation to Rice University.

**Reprints:** José A. López, Thrombosis Research Section, Department of Medicine, BCM286, N1319, Baylor College of Medicine, 1 Baylor Plaza, Houston, TX 77030; e-mail: josel@bcm.tmc.edu.

The publication costs of this article were defrayed in part by page charge payment. Therefore, and solely to indicate this fact, this article is hereby marked "advertisement" in accordance with 18 U.S.C. section 1734.

of both GP Ib-IX-V complexes[12] and VWF multimers,[13] although the precise mechanism by which shear induces the interaction is unknown. In the absence of high shear stress, the exogenous modulators ristocetin or botrocetin are required for the binding of plasma VWF to GP Ib-IX.

It has been presumed that the interaction of VWF with GP Ib-IX complexes on platelets is governed predominantly by its multimeric size.[14] To address this question, we used optical tweezers to investigate the interaction of GP Ib-IX with the different forms of VWF: plasma VWF, ULVWF, and isolated A1 domain. We demonstrate that, unlike plasma VWF, ULVWF requires no modulators to bind the GP Ib-IX complex, and the minimal strength of its bond to the GP Ib-IX complex is 1.5 times that of the plasma VWF–GP Ib-IX bond in the presence of modulator and similar to the A1–GP Ib-IX bond. These findings suggest that the conformational state of VWF multimers may be more critical than their multimeric size in the VWF–GP Ib-IX interaction.

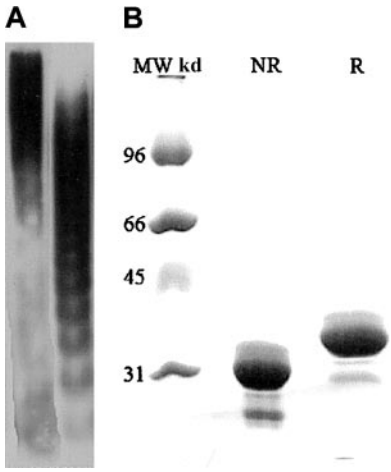


**Figure 1. ULVWF, plasma VWF, and A1 domain samples displayed by gel electrophoresis.** (A) The histamine-stimulated endothelial cell supernatant contains ULVWF multimers (first lane). ULVWF multimers are absent in the plasma VWF sample (second lane). The VWF-to-antigen levels for ULVWF and plasma VWF were 15 U/dL and 100 U/dL, respectively. Analysis of ULVWF and plasma VWF was by sodium dodecyl sulfate (SDS)–polyacrylamide gel electrophoresis (12.5%) and chemiluminescence. (B) The first lane contains molecular weight markers. Under reducing (R) and nonreducing (NR) conditions, the VWF A1 domain exists as a 36-kd monomer (second and third lanes). The reducing agent was 2-mercaptoethanol. VWF A1 concentrations used were 100 and 200 μg/mL. Analysis of the A1 domain was by SDS-agarose (1%) electrophoresis and autoradiography.

## Materials and methods

### Cells expressing GP Ib-IX complexes.

In our initial experiments, we found that investigation of the VWF–GP Ibα interaction using platelets produced inconsistent results because platelets express other receptors that bind VWF in addition to the GP Ib-IX-V complex. Therefore, we used Chinese hamster ovary (CHO) cells that stably express GP Ib-IX complexes to examine the binding strength between membrane-bound GP Ib-IX complexes and polystyrene bead–bound VWF multimers. These cells (CHO αβIX) have been previously used to characterize the shear-dependent interaction between the GP Ib-IX complex and VWF by means of a parallel-plate flow chamber.[15-17] The GP V subunit is not required for the VWF–GP Ibα interaction, and we did not include it in our transfection system. CHO βIX cells, which express GP Ibβ and GP IX but not GP Ibα, do not bind VWF and were used as a negative control.

### Preparation of VWF and VWF-coated beads

The interactions of plasma VWF, ULVWF, and A1 domain with GP Ib-IX were investigated. The VWF multimers containing all of the multimeric forms present in normal plasma were purified from the cryoprecipitate fraction of normal human plasma by glycine and NaCl precipitation, followed by separation on a Sepharose 4B column.[11,18] The purified VWF was then equilibrated to 100% and 1000% of normal human plasma concentration (approximately 10 and approximately 100 μg/mL, respectively) in citrate phosphate buffer consisting of 0.0394 M citric acid and 0.1212 M dibasic sodium phosphate. Multimers enriched in ULVWF forms were obtained from the supernatant of histamine-stimulated human umbilical vein endothelial cells as previously described.[11] Most of the VWF found in the endothelial cell supernatant is of very high molecular weight, above that of the largest plasma VWF multimers. Representative gels of the plasma VWF and ULVWF multimers are shown in Figure 1A. Recombinant VWF A1 domain was produced by a previously described method,[19] and a representative gel of the domain is shown in Figure 1B.

Polystyrene beads (Polysciences, Warrington, PA) with a diameter of 2.0 μm were coated with VWF according to the following procedure. Single drops of bead suspensions were added to tubes containing VWF at a concentration of either approximately 10 or approximately 100 μg/mL in citrate phosphate buffer. The beads and either purified VWF or ULVWF multimers were then incubated for 1 hour at room temperature with gentle mixing on an aliquot shaker. The suspension was subsequently centrifugued for 2 minutes in an Eppendorf microcentrifuge at 15 000 rpm. The supernatant was removed, and the beads were resuspended by vortex in Dulbecco phosphate-buffered saline (PBS) solution (pH, 7.3) containing 10 mg/mL bovine serum albumin, 1 mg/mL sodium azide, and 5% glycerol. The beads were then washed in 1 mL Dulbecco PBS solution, incubated for 30 minutes, centrifuged for 2 minutes, and resuspended in 0.5 mL Dulbecco PBS solution.

### Monoclonal antibody

The monoclonal antibody AK2 binds to GP Ibα and completely blocks VWF binding to GP Ib.[20] To verify that we were specifically investigating the VWF–GP Ib-IX interaction, the CHO cells in the solution chamber were preincubated for 20 minutes with AK2 before the adhesion assays.

### Modulators

The compounds botrocetin and ristocetin were used to induce binding between plasma VWF and GP Ib-IX. Botrocetin is a 25-kd dimeric protein purified from the venom of the South American pit viper *Bothrops jararca*. Botrocetin forms a complex with VWF by binding near the GP Ib–binding site.[21] Ristocetin is an antibiotic glycopeptide synthesized by *Nocardia lurida* thought to interact with both GP Ib-IX and VWF,[22] although the mechanism by which it induces the VWF–GP Ib-IX interaction remains unclear.

### Optical tweezers

Damage to cells induced by light varies with the incident wavelength, but little or no damage has been demonstrated at 830 nm in an optical trap.[23] We used a titanium-sapphire laser tuned to 830 nm (Model 3900 S; Spectra-Physics, Santa Clara, CA) in our optical tweezers setup (Figure 2). The titanium-sapphire laser was pumped by a solid-state, frequency-doubled neodynium yttrium vanadate (Nd:$YVO_4$) laser operating at a wavelength of 532 nm (Millennia V; Spectra-Physics). The laser beam was expanded (CM cwbx-7.0-s-670/1064; Spectra-Physics) 5-fold to fill the back aperture of the microscope objective (numerical aperture 1.3). The laser light then passed through an attenuator (Model 925B; Newport Electronics, Irvine, CA) used to control the beam intensity. A dichroic mirror placed just before the bottom entrance port transmitted the laser light into the microscope (Axiovert S100TV; Carl Zeiss, Jena, Germany) and reflected the light below 650 nm toward a beam splitter, which transmitted 10% of the light to a charged-coupled device (CCD) camera (Model CCD 100; DAGE–MTI, Michigan City, IN) for imaging purposes. The solution chamber containing cells was mounted onto a piezoelectrically driven translational stage (Model P-527.3CL; Physik Instrumente, Waldbronn, Germany). The cell

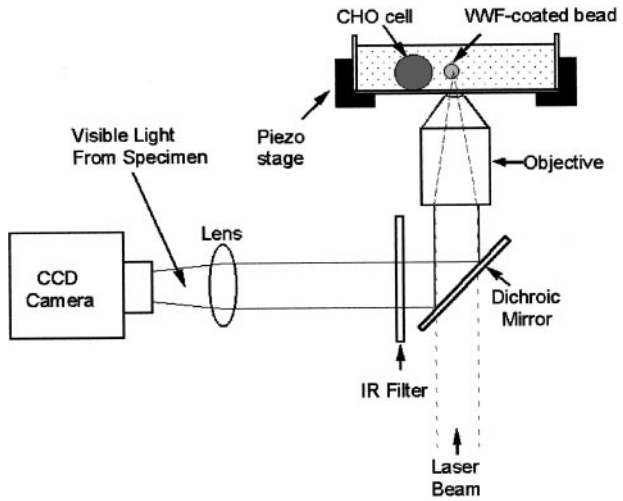


**Figure 2. Optical tweezers setup.** Light from a titanium-sapphire laser (λ = 830 nm) is reflected by a dichroic mirror and is focused onto the objective lens of the inverted microscope to trap the bead. A charged-coupled device (CCD) camera collects 10% of the light for image visualization. The CHO cell and VWF-coated bead are in a solution chamber mounted onto a piezoelectrically driven translational stage.

chamber was illuminated from the top with white light for visualizing the specimens.

### Calibration procedure

The optical trapping force was calibrated by moving a solution past a trapped bead at a known velocity with the use of the piezoelectric stage and calculating the force required to displace the bead from the trap using the Stokes law,

$$f = \frac{6\pi\eta v r}{1 - \frac{9}{16}\left(\frac{r}{h}\right) + \frac{1}{8}\left(\frac{r}{h}\right)^3 - \frac{45}{256}\left(\frac{r}{h}\right)^4 - \frac{1}{16}\left(\frac{r}{h}\right)^5}$$

where $\eta$ is the solution viscosity (1 cP), $v$ is the solution velocity, $r$ is the bead radius, and $h$ is the distance between the center of the bead and the coverslip.[24]

For a given laser power, the bead will eventually escape the trap when the drag force exerted by the fluid exceeds the trapping force. The drag force at which the bead escapes from the trap is the escaping force, and was determined over a range of laser powers measured past the microscope objective lens. Figure 3 shows the escaping force as a function of laser power for a 2.0-μm polystyrene bead placed at a height of 10 μm from the coverslip ($h$ = 10 μm). The system was calibrated at a height of 10 μm since the VWF-coated bead is in contact with the CHO cell approximately 10 μm from the coverslip during the experiments. There was a linear relationship between the escaping force and laser power with a slope of approximately 0.9 pN/mW.

### Interaction of VWF and GP Ib-IX complexes

We optically trapped a 2.0-μm bead coated with VWF and moved the transfected CHO cell toward the trapped bead by using the piezoelectrically driven stage. Initial binding between plasma VWF and GP Ib-IX was induced by the addition of either 1 mg/mL ristocetin or 2 μg/mL botrocetin to the solution chamber. The CHO cell was placed in the solution chamber 20 minutes before an experiment to allow it to adhere firmly to the coverslip. The VWF-coated bead was placed into contact with the cell and allowed to remain there for 10 seconds. Adhesion times up to 90 seconds between the bead and the cell were also examined. Following adhesion, the laser power was reduced by adjusting the attenuator to the minimum level required to trap the VWF-coated bead.

To determine bond strength, we attempted to detach the cell from the bead by moving the piezoelectric stage. If the cell could not be detached from the bead, the laser power was incrementally increased, and another attempt was made to detach the bead from the cell. This process was repeated until the minimum laser power required to detach the VWF-coated bead from the CHO cell was determined. The minimum optical power required to detach the bead was converted to a force value that represented the bond strength of the VWF–GP Ib-IX interaction by means of the calibration curve. To induce the formation of multiple bonds, the VWF-coated bead was forcefully pushed against the cell and subsequently detached after 10 seconds of adhesion. After measuring the forces required to detach the coated bead from the cell, we observed distinct groups of data points whose cluster means were integral multiples of putative single-bond strengths for each ligand–receptor interaction studied.

### Interactions of modulators with VWF

Polystyrene beads ($r$ = 2.25 μm) were coated with ristocetin or botrocetin, and smaller beads ($r$ = 1.0 μm) were coated with plasma VWF in order to determine whether the modulators were detaching from the VWF. The modulator-coated bead was first allowed to adhere firmly to the coverslip for 20 minutes. We then trapped the VWF-coated bead and allowed it to bind to the modulator-coated bead for 10 seconds. The force to detach the VWF-coated bead from the modulator-coated bead was then determined as described above.

### Statistics

Each result is reported as the mean ± SD. Student $t$ test was used to evaluate differences between the mean values of the putative single-bond strengths for GP Ib-IX and its ligands.

## Results

A bond was considered to have formed if the force needed to retract the VWF-coated bead from the CHO cell was greater than the force needed to move the bead in solution in the absence of CHO cells. In the absence of ristocetin or botrocetin, no adhesion was detected between plasma VWF–coated beads and CHO αβIX cells. Similarly, no adhesion was detectable in the presence of the GP Ibα monoclonal antibody AK2, regardless of whether a modulator was used. In addition, no adhesion was observed between the CHO βIX cells (expressing GP Ibβ and GP IX, but not GP Ibα) and the beads coated with plasma VWF, ULVWF, or A1 domain. The sequence of a typical experiment consisting of adhesion of the VWF-coated bead to the CHO αβIX cell and subsequent detachment is shown in Figure 4.

### Ristocetin-induced binding of purified plasma VWF to CHO αβIX cells

Bonds formed between the beads coated with purified plasma VWF and the CHO αβIX cells only in the presence of either ristocetin or

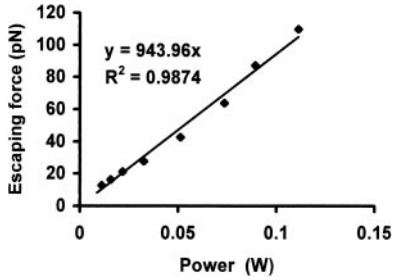


**Figure 3. Escaping force as a function of laser power after objective lens for a 2.0-μm polystyrene bead was placed at a height of 10 μm from the coverslip.** There was a linear relationship between the escaping force and laser power, with a slope of approximately 0.9 pN/mW.

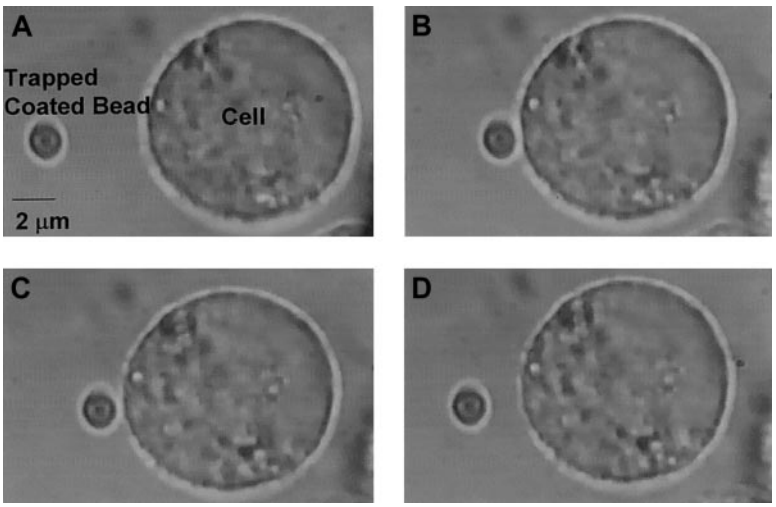


**Figure 4. Bead adhesion and subsequent detachment from CHO cell.** (A) The VWF-coated bead is optically trapped, and the CHO αβIX cell is moved toward the bead. (B) The bead adheres to cell for 10 seconds. (C) After laser power is increased, the bead begins to detach. (D) The bead is fully detached. Original magnification × 100.

botrocetin. In the presence of ristocetin, the force necessary to break the bonds occurred in integer multiples of the putative single-bond strength, 6.5 ± 0.8 pN, depending upon the number of bonds initially formed (Figure 5). With beads coated at a higher VWF density, more bonds formed on average. Nevertheless, the value for a single bond was the same as with beads coated at lower density (Figure 5B).

### Botrocetin-induced plasma VWF binding to CHO αβIX cells

The single-bond strength for the botrocetin-induced attachment of plasma VWF to GP Ib-IX was 8.8 ± 0.3 pN. As with ristocetin-induced binding, the higher measured values were integer multiples of this single-bond strength (Figure 6). More bonds formed with beads coated at a higher density of plasma VWF, but the single-bond value remained the same (Figure 6B).

### Ristocetin and botrocetin adhesion to VWF

To ensure that neither botrocetin nor ristocetin was being detached from VWF during the experiments, we measured the unbinding forces between plasma VWF–coated beads and beads coated with either botrocetin or ristocetin. It was not possible to detach the 2 spheres, whether the modulator was ristocetin or botrocetin, even at maximum laser power.

### Binding of ULVWF to CHO αβIX cells

We performed 100 binding assays. In each, a different bead and a different cell were used. Unlike plasma VWF–coated beads, all of the ULVWF-coated beads bound CHO αβIX cells spontaneously, without the need for ristocetin or botrocetin. The ULVWF–GP Ib-IX single-bond strength was 11.4 ± 2.1 pN. Higher measured values were integral multiples of this value (Figure 7). At higher ULVWF-coating densities, more bonds tended to form; the strength of the single bond was again identical with that found at lower ULVWF-coating density.

### Binding of the VWF A1 domain to CHO αβIX cells

Beads coated with purified Al domain were also able to bind CHO αβIX cells in the absence of modulators, with a single-bond strength of approximately 11.5 pN per bond (Figure 8), virtually identical to that observed for the interaction of ULVWF with the CHO αβIX cells.

### Statistics

The mean single-bond strengths of the interactions between the GP Ib-IX complex and each of the different forms of VWF (plasma, ULVWF, and the A1 domain) were compared by means of the Student *t* test. The ULVWF–GP Ib-IX and A1–GP Ib-IX bond strengths were not significantly different ($P = .7414$). The remaining bond strengths were significantly different ($P < .05$) when compared with each other.

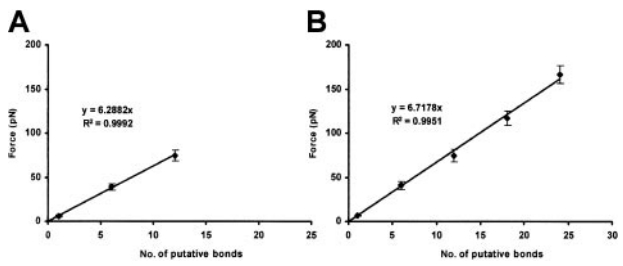


**Figure 5. Ristocetin-dependent plasma VWF–GP Ib-IX binding.** Plots show the cumulative results of detachment of plasma VWF–coated beads (10 and 100 μg/mL VWF concentration; panels A and B, respectively) from CHO αβIX cells in the presence of ristocetin (1 mg/mL). Although the slopes are similar, more VWF/GP Ib-IX bonds are formed when the 100 μg/mL VWF concentration is used (panel B). Data in each panel represent the mean values of 200 bead-cell detachments.

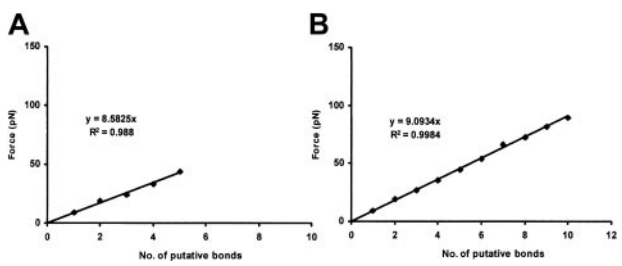


**Figure 6. Botrocetin-dependent plasma VWF–GP Ib-IX binding.** Plots show the cumulative results of detachment of plasma VWF-coated beads (10 and 100 μg/mL VWF concentration; panels A and B, respectively) from CHO αβIX cells in the presence of botrocetin (2.5 μg/mL). Although the slopes are similar, more VWF/GP Ib-IX bonds are formed when the 100 μg/mL VWF concentration is used (panel B). Data in each panel represent the mean values of 120 bead-cell detachments.

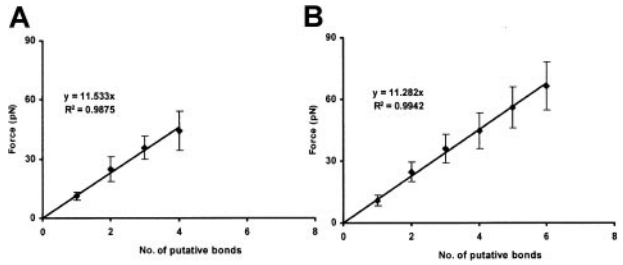


**Figure 7. ULVWF–GP Ib-IX binding.** Plots show the cumulative results of detachment of ULVWF-coated beads (10 and 100 μg/mL ULVWF concentration; panels A and B, respectively) from CHO αβIX cells. Although the slopes are similar, more VWF/GP Ib-IX bonds are formed when the 100 μg/mL VWF concentration is used (panel B). Data in each panel represent the mean values of 40 and 60 bead-cell detachments, respectively.

## Discussion

The interaction between the platelet GP Ib-IX-V complex and VWF is the initiating event of platelet adhesion. This interaction normally does not occur in the fluid phase, unless induced by extremely high shear stresses.[3] When bound VWF is exposed on the subendothelium, however, it is able to interact with the GP Ib-IX-V complex and thus to capture platelets from the flowing blood, a process that becomes more efficient with increasing shear stress.[25] Considerable evidence exists that unprocessed forms of ULVWF are more efficient at binding platelets and are capable of binding platelets spontaneously. This spontaneous binding, with subsequent aggregation of the platelets, is the presumed pathophysiology of the catastrophic arterial thrombotic disorder, thrombotic thrombocytopenic purpura (TTP), which is characterized pathologically by extensive microvascular occlusion with thrombi composed almost entirely of platelets and VWF. TTP is believed to be caused by deficiency of a recently characterized protease of the disintegrin and metalloproteinase domain, with thrombospondin type–1 modules (ADAMTS) family (ADAMTS13),[26-29] which is responsible for the proteolytic processing of the ULVWF to less reactive plasma forms.

Although the interaction between the GP Ib-IX-V complex and VWF has been extensively studied, the basis of the increased reactivity of ULVWF remained a mystery. It has been presumed that multimeric size was the main determinant of the reactivity of the ultralarge multimers, partially on the basis of the increased propensity for bleeding observed when the larger plasma forms are missing in types 2A and 2B von Willebrand disease and in platelet-type von Willebrand disease.[25,30] This hypothesis has never been tested directly, primarily because of the difficulty of isolating single ligand–receptor bonds (by single bond, we mean here the minimum stoichiometry of ligand and receptor capable of producing a measurable bond). We were able to overcome this technical obstacle in the current studies with the use of optical tweezers. This technique allowed us to compare in detail the interaction of the GP Ib-IX complex with the different forms of VWF, and to do so at the level of single-bond units.

Our results reveal a fundamental difference at the level of single bonds between unprocessed ULVWF and VWF purified from plasma. Whereas the plasma VWF required the modulators ristocetin or botrocetin to bind cells expressing the GP Ib-IX complex, ULVWF bound the cells spontaneously, without modulators. In addition, the strength of the individual bond between VWF and the GP Ib-IX complex was more than 1.3 times greater for ULVWF than for plasma VWF in the presence of either modulator. Thus, not only is ULVWF of much higher molecular weight on average than plasma VWF; it is inherently stickier. Processing ULVWF to a less adhesive form is thus part of the normal physiological role of the ADAMTS13 protease. Of great relevance to our attempts to understand the nature of the processing step was our finding that the strength of the individual bonds formed between ULVWF and GP Ib-IX was virtually identical to the strength of the bonds formed between the GP Ib-IX complex and the isolated A1 domain. Thus, it appears that not only does unprocessed ULVWF exist, on average, in a form of higher molecular weight, but its GP Ibα–binding A1 domain also appears to be exposed for binding. It was not possible to determine what percentage of the total A1 domains in a VWF multimer exists in the exposed conformation in ULVWF.

These studies also raise the possibility that one reason for the observed difference in binding between plasma VWF and VWF immobilized on the subendothelium is that the latter form may not have undergone complete processing before it binds platelets, perhaps because it was secreted abluminally to a compartment inaccessible to the plasma protease. Such a scenario would provide an elegant mechanism by which subendothelial VWF could bind platelets efficiently, while the plasma forms remain relatively unreactive. Of interest, plasma VWF can mediate the attachment and rolling of platelets when coated onto a glass surface, but the relationship of this interaction to that of platelets with subendothelial VWF in vivo is unknown.

Several studies have used optical tweezers to examine receptor-ligand relationships in biological systems. For example, Liang et al[31] examined adhesion of *Escherichia coli* to mannose-presenting surfaces. In that study, integral multiples of 1.7 pN were reported to represent the force to detach one molecule of α-C-mannoside from the bacterium. With the use of optical tweezers, the actin-myosin unbinding force has been determined to be approximately 9 pN,[32] which is remarkably close to the value we determined for the interaction of plasma VWF with the GP Ib-IX complex in the presence of ristocetin. This is not unexpected, particularly since neither the actin-myosin interaction nor the VWF–GP Ib-IX interaction is associated with irreversible adhesion. The unbinding and rebinding of actin and myosin are the crucial steps for the sliding movement in muscle that allows contraction. Likewise, the VWF–GP Ib-IX interaction is associated with platelets that are tethered to the vessel wall and that move in the direction of the flow. As the platelets translocate along the vessel wall, they become activated, partly through this interaction and partly through the interaction of other platelet receptors with collagen.[33] While the VWF–GP Ib-IX bond must be strongly resistant to tensile stress, the bond nevertheless has a high dissociation rate.[34] Thus, it comes as no surprise that the VWF–GP Ib-IX bond is significantly weaker

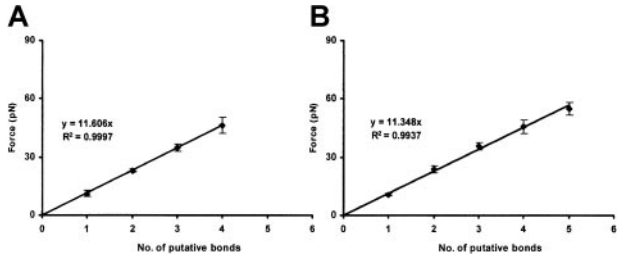


**Figure 8. A1 domain–GP Ib-IX binding.** Plots show the cumulative results of detachment of A1-coated beads (100 and 200 μg/mL A1 concentration; panels A and B, respectively) from CHO αβIX cells. Although the slopes are similar, more A1/GP Ib-IX bonds are formed when the 200 μg/mL VWF concentration is used (panel B). Each panel represents the mean values of 30 bead-cell detachments.

than bonds associated with firm adhesion, such as the $\alpha_V\beta_3$ integrin–echistatin interaction, which has been reported to be approximately 100 pN per bond.[35]

In addition to helping us distinguish between plasma VWF and ULVWF, the optical tweezer technique allowed us to compare the bonds induced by botrocetin and ristocetin. The 2 modulators induce the interaction by fundamentally different mechanisms, and this is borne out by our data, which demonstrate that the modulators induce bonds of different strengths between plasma VWF and the GP Ib-IX complex. These studies also preclude the possibility that we were dissociating the interaction between the modulator and VWF, as the VWF-coated beads formed much stronger bonds with beads coated with either ristocetin or botrocetin than they did with GP Ib-IX complex–expressing cells. The difference in binding strength induced between the 2 modulators and the yet stronger binding of ULVWF- or A1-coated beads also excludes the possibility that the forces being measured were those required to extract the GP Ib-IX complex from the cell membrane.

Other investigators have determined that ristocetin binds to both VWF and GP Ib, thereby facilitating adhesion between the receptor and its ligand.[36] The results of the ristocetin-dependent plasma VWF/GP Ib-IX–binding experiments are quite intriguing since our lowest force measurement is 6.5 pN while the subsequent value is 39 pN, exactly 6 times the initial value. The higher bond strength values all increased in integer multiples of 39 pN. This pattern of increase in the force measurement stands in stark contrast to the stepwise increase from the minimal value in the botrocetin-mediated VWF/GP Ib-IX force data. This raises the possibility that the true single-bond strength for the ristocetin-induced VWF/GP Ib-IX bond is approximately 39 pN. While the exact mechanism of ristocetin-induced binding of VWF to GP Ib is not known, some have suggested that ristocetin binds to GP Ib through 4 ristocetin monomers or through 2 ristocetin dimers.[22] While 2 ristocetin dimers could indeed act as a bridge between VWF and GP Ib, it is also possible that multiple ristocetin dimers, perhaps 6, could facilitate the VWF/GP Ib interaction. Future experiments using the optical tweezers will allow us to address the nature of the ristocetin-dependent VWF/GP Ib bond.

In summary, we have used optical tweezers to compare the strength of the interactions between different forms of VWF and the platelet GP Ib-IX complex. These studies confirm the notion that the modulators ristocetin and botrocetin differ in the nature of the bond they induce between the ligand and the receptor. The studies have also allowed us to examine the basis of the enhanced reactivity with platelets observed for ULVWF as compared with the usual plasma forms of VWF, revealing that ULVWF is inherently more adhesive for platelets than is plasma VWF. This finding may shed some light on the pathophysiology of the thrombotic microangiopathies.

## Acknowledgments

We thank Ms Nancy Turner and Ms Letty Nolasco for preparation of the VWF and ULVWF, and Mr Zhiwei Li, Ms Kathryn Simpson, and Dr Jorge Torres for invaluable assistance with the optical tweezers.

## References

1. Lopez JA. The platelet glycoprotein Ib-IX complex. Blood Coagul Fibrinolysis. 1994;5:97-119.
2. Weiss HJ. Flow-related platelet deposition on subendothelium. Thromb Haemost. 1995;74:117-122.
3. Kroll MH, Hellums JD, McIntire LV, Schafer AI, Moake JL. Platelets and shear stress. Blood. 1996;88:1525-1541.
4. Andrews RK, Lopez JA, Berndt MC. Molecular mechanisms of platelet adhesion and activation. Int J Biochem Cell Biol. 1997;29:91-105.
5. Ruggeri ZM. Mechanisms initiating platelet thrombus formation. Thromb Haemost. 1997;78:611-616.
6. Sadler JE. Biochemistry and genetics of von Willebrand factor. Annu Rev Biochem. 1998;67:395-424.
7. Mayadas TN, Wagner DD. von Willebrand factor biosynthesis and processing. Ann N Y Acad Sci. 1991;614:153-166.
8. Moake JL. von Willebrand factor in the pathophysiology of thrombotic thrombocytopenic purpura. Clin Lab Sci. 1998;11:362-364.
9. Olson JD, Moake JL, Collins MF, Michael BS. Adhesion of human platelets to purified solid-phase von Willebrand factor: studies of normal and Bernard-Soulier platelets. Thromb Res. 1983;32:115-122.
10. Moake JL, Turner NA, Stathopoulos NA, Nolasco L, Hellums JD. Shear-induced platelet aggregation can be mediated by vWF released from platelets, as well as by exogenous large or unusually large vWF multimers, requires adenosine diphosphate, and is resistant to aspirin. Blood. 1988;71:1366-1374.
11. Moake JL, Turner NA, Stathopoulos NA, Nolasco LH, Hellums JD. Involvement of large plasma von Willebrand factor (vWF) multimers and unusually large vWF forms derived from endothelial cells in shear stress-induced platelet aggregation. J Clin Invest. 1986;78:1456-1461.
12. Peterson DM, Stathopoulos NA, Giorgio TD, Hellums JD, Moake JL. Shear-induced platelet aggregation requires von Willebrand factor and platelet membrane glycoproteins Ib and IIb-IIIa. Blood. 1987;69:625-628.
13. Bolhuis PA, Sakariassen KS, Sander HJ, Bouma BN, Sixma JJ. Binding of factor VIII-von Willebrand factor to human arterial subendothelium precedes increased platelet adhesion and enhances platelet spreading. J Lab Clin Med. 1981; 97:568-576.
14. Furlan M. Von Willebrand factor: molecular size and functional activity. Ann Hematol. 1996;72: 341-348.
15. Fredrickson BJ, Dong JF, McIntire LV, Lopez JA. Shear-dependent rolling on von Willebrand factor of mammalian cells expressing the platelet glycoprotein Ib-IX-V complex. Blood. 1998;92:3684-3693.
16. Dong JF, Li CQ, Lopez JA. Tyrosine sulfation of the glycoprotein Ib-IX complex: identification of sulfated residues and effect on ligand binding. Biochemistry. 1994;33:13946-13953.
17. Dong JF, Hyun W, Lopez JA. Aggregation of mammalian cells expressing the platelet glycoprotein (GP) Ib-IX complex and the requirement for tyrosine sulfation of GP Ib alpha. Blood. 1995; 86:4175-4183.
18. Thorell L, Blomback B. Purification of the factor VIII complex. Thromb Res. 1984;35:431-450.
19. Cruz MA, Handin RI, Wise RJ. The interaction of the von Willebrand factor-A1 domain with platelet glycoprotein Ib/IX. The role of glycosylation and disulfide bonding in a monomeric recombinant A1 domain protein. J Biol Chem. 1993;268:21238-21245.
20. Ward CM, Andrews RK, Smith AI, Berndt MC. Mocarhagin, a novel cobra venom metalloproteinase, cleaves the platelet von Willebrand factor receptor glycoprotein Ibalpha: identification of the sulfated tyrosine/anionic sequence Tyr-276-Glu-282 of glycoprotein Ibalpha as a binding site for von Willebrand factor and alpha-thrombin. Biochemistry. 1996;35:4929-4938.
21. Sugimoto M, Mohri H, McClintock RA, Ruggeri ZM. Identification of discontinuous von Willebrand factor sequences involved in complex formation with botrocetin: a model for the regulation of von Willebrand factor binding to platelet glycoprotein Ib. J Biol Chem. 1991;266:18172-18178.
22. Hoylaerts MF, Nuyts K, Peerlinck K, Deckmyn H, Vermylen J. Promotion of binding of von Willebrand factor to platelet glycoprotein Ib by dimers of ristocetin. Biochem J. 1995;306(Pt 2):453-463.
23. Neuman KC, Chadd EH, Liou GF, Bergman K, Block SM. Characterization of photodamage to Escherichia coli in optical traps. Biophys J. 1999; 77:2856-2863.
24. Happel J, Brenner H. Low Reynolds Number Hydrodynamics. Dordrecht, The Netherlands: Kluwer Academic; 1991.
25. Lopez JA, Andrews RK, Afshar-Kharghan V, Berndt MC. Bernard-Soulier syndrome. Blood. 1998;91:4397-4418.
26. Fujikawa K, Suzuki H, McMullen B, Chung D. Purification of human von Willebrand factor-cleaving protease and its identification as a new member of the metalloproteinase family. Blood. 2001;98: 1662-1666.
27. Gerritsen HE, Robles R, Lammle B, Furlan M. Partial amino acid sequence of purified von Willebrand factor-cleaving protease. Blood. 2001;98: 1654-1661.
28. Levy GG, Nichols WC, Lian EC, et al. Mutations

in a member of the ADAMTS gene family cause thrombotic thrombocytopenic purpura. Nature. 2001;413:488-494.

29. Zheng X, Chung D, Takayama TK, Majerus EM, Sadler JE, Fujikawa K. Structure of von Willebrand factor-cleaving protease (ADAMTS13), a metalloprotease involved in thrombotic thrombocytopenic purpura. J Biol Chem. 2001;276: 41059-41063.
30. Sadler JE, Mannucci PM, Berntorp E, et al. Impact, diagnosis and treatment of von Willebrand disease. Thromb Haemost. 2000;84:160-174.
31. Liang MN, Smith SP, Metallo SJ, Choi IS, Prentiss M, Whitesides GM. Measuring the forces involved in polyvalent adhesion of uropathogenic Escherichia coli to mannose-presenting surfaces. Proc Natl Acad Sci U S A. 2000;97:13092-13096.
32. Nishizaka T, Miyata H, Yoshikawa H, Ishiwata S, Kinosita K Jr. Unbinding force of a single motor molecule of muscle measured using optical tweezers. Nature. 1995;377:251-254.
33. Clemetson KJ, Clemetson JM. Platelet collagen receptors. Thromb Haemost. 2001;86:189-197.
34. Ruggeri ZM. von Willebrand factor. J Clin Invest. 1997;99:559-564.
35. Lehenkari PP, Horton MA. Single integrin molecule adhesion forces in intact cells measured by atomic force microscopy. Biochem Biophys Res Commun. 1999;259:645-650.
36. Scott JP, Montgomery RR, Retzinger GS. Dimeric ristocetin flocculates proteins, binds to platelets, and mediates von Willebrand factor-dependent agglutination of platelets. J Biol Chem. 1991;266: 8149-8155.